Electronic Supplementary Material (ESI) for Energy & Environmental Science.

Supplementary Materials

Solar desalination charger for water treatment and value-added chemical production

Seonghun Kim,[1] Dong Suk Han,[2] and Hyunwoong Park[1,*]

[1]*School of Energy Engineering, Kyungpook National University, Daegu 41566, Korea*

[2]*Center for Advanced Materials, Qatar University, Doha 2713, Qatar*

* To whom correspondence should be addressed (H. Park)

E-mail: hwp@knu.ac.kr; Tel: +82-53-950-8973

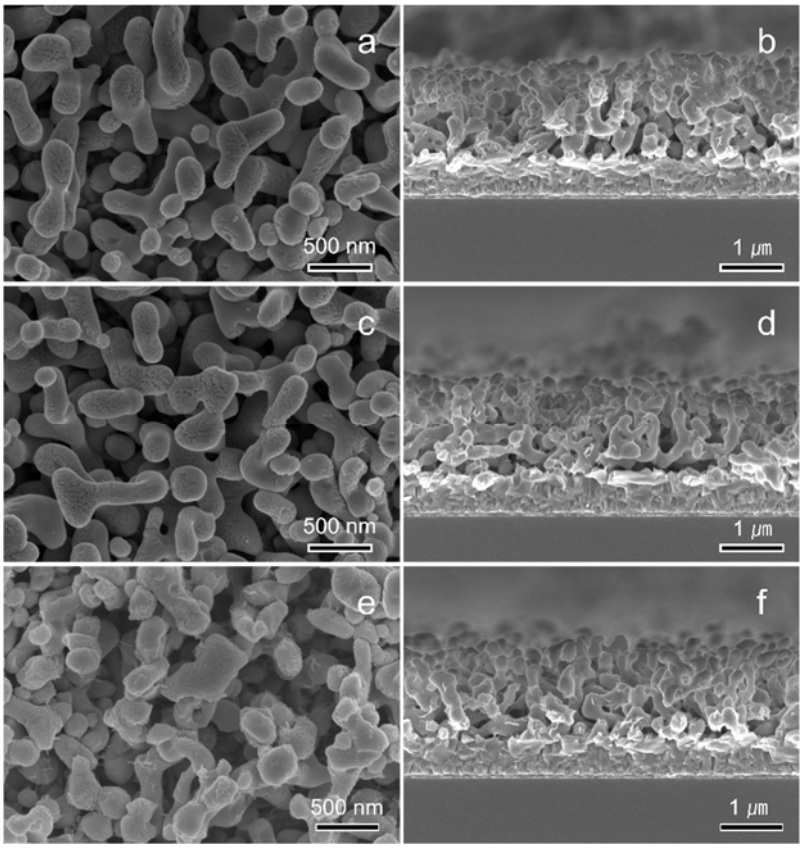

Fig. S1. FE-SEM images of (a and b) BVO, (c and d) WBVO, and (e and f) Co-WBVO.

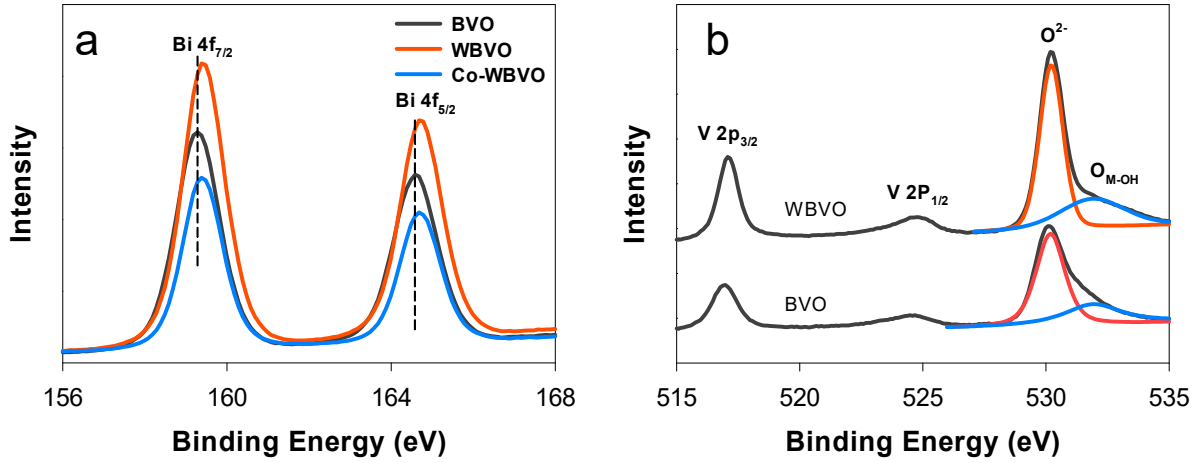

Fig. S2. XPS spectra of Bi 4f, V 2p, and O 1s bands for BVO and WBVO samples.

Table S1. Photoelectrocatalytic chloride oxidation activities using various photoanodes

Sample	Potential (V)	J_{ph} (mA cm^{-2})	Electrolyte	Light source (mW cm^{-2})	FE_{ClOR} (%)	Ref.
$BiVO_4/WO_3$	1.4 V	1.25	5 M NaCl	100 mW cm^{-2} L-42 cutoff filter	81.4	[1]
$BiVO_4/WO_3$	1.42 V_{RHE}	2.61	4 M NaCl, pH 1	100 mW cm^{-2}	74	[2]
WO_3	1.46 V_{RHE}	4.78	Synthetic seawater	100 mW cm^{-2}	70	[3]
Co doped $BiVO_4$	1.1 V_{RHE}	0.19	1 M NaCl, pH 2.3	100 mW cm^{-2}	92	[4]
CoOx-loaded $BiVO_4/WO_3$	1.0 V_{RHE}	1	0.5 M NaCl	100 mW cm^{-2} L-42 cutoff filter	95	[5]
$BiVO_4$	1.36 V_{RHE}	1.45	0.171 M NaCl	100 mW cm^{-2}	40	This work
W-$BiVO_4$		2.4			48	This work
W-$BiVO_4$ / CoOOH		3.55			91	This work

References

1. Iguchi, S., Y. Miseki, and K. Sayama, *Efficient hypochlorous acid (HClO) production via photoelectrochemical solar energy conversion using a $BiVO_4$-based photoanode.* Sustainable Energy & Fuels, 2018. **2**(1): p. 155-162.
2. Rassoolkhani, A.M., et al., *Nanostructured bismuth vanadate/tungsten oxide photoanode for chlorine production with hydrogen generation at the dark cathode.* Communications Chemistry, 2019. **2**(1): p. 57.
3. Jadwiszczak, M., et al., *Highly efficient sunlight-driven seawater splitting in a photoelectrochemical cell with chlorine evolved at nanostructured WO_3 photoanode and hydrogen stored as hydride within metallic cathode.* Advanced Energy Materials, 2020. **10**(3): p. 1903213.
4. Chauhan, I., et al., *Nanostructured Co-doped $BiVO_4$ for efficient and sustainable photoelectrochemical chlorine evolution from simulated sea-water.* Dalton Trans, 2023.
5. Okunaka, S., Y. Miseki, and K. Sayama, *Improvement of photoelectrochemical HClO production under visible light irradiation by loading cobalt oxide onto a $BiVO_4$ photoanode.* Catalysis Science & Technology, 2021. **11**(16): p. 5467-5471.

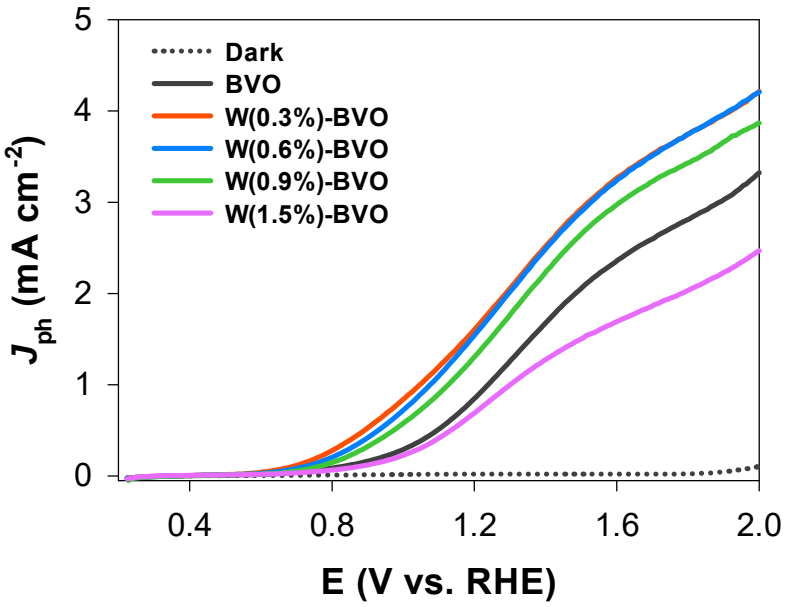

Fig. S3. Linear sweep voltammograms with BVO and W-doped BVO in 0.171 M NaCl solution in the dark and under 1 sun.

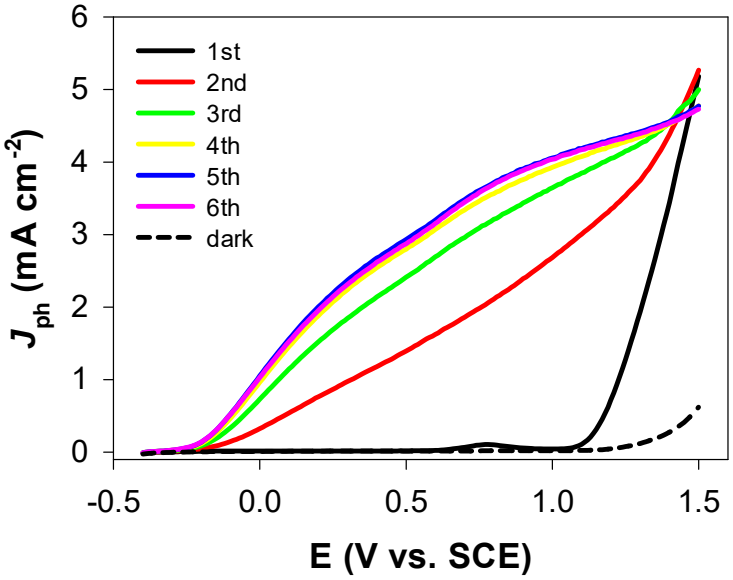

Fig. S4. Repetitive linear sweep voltammograms with Co-WBVO in 0.171 M NaCl in the dark and under 1 sun.

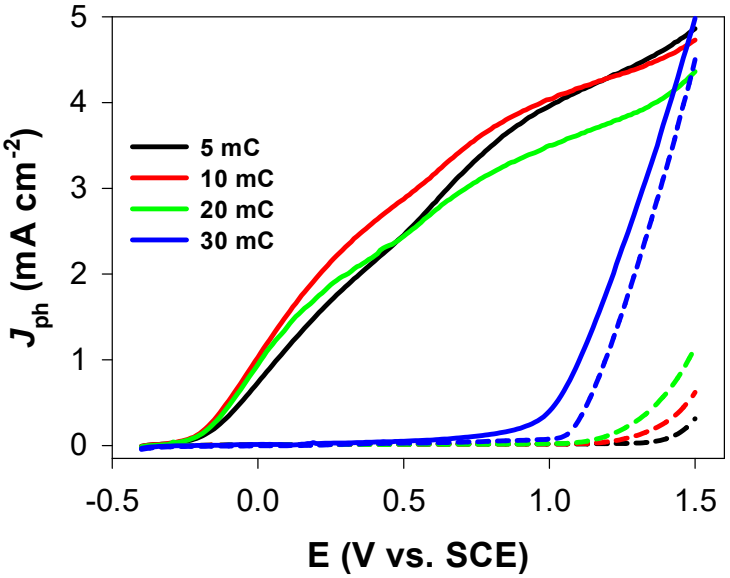

Fig. S5. Linear sweep voltammograms with Co-WBVO as a function of Co-electrodeposition charges on WBVO in 0.171 M NaCl solution in the dark (dashed curves) and under 1 sun (solid curves).

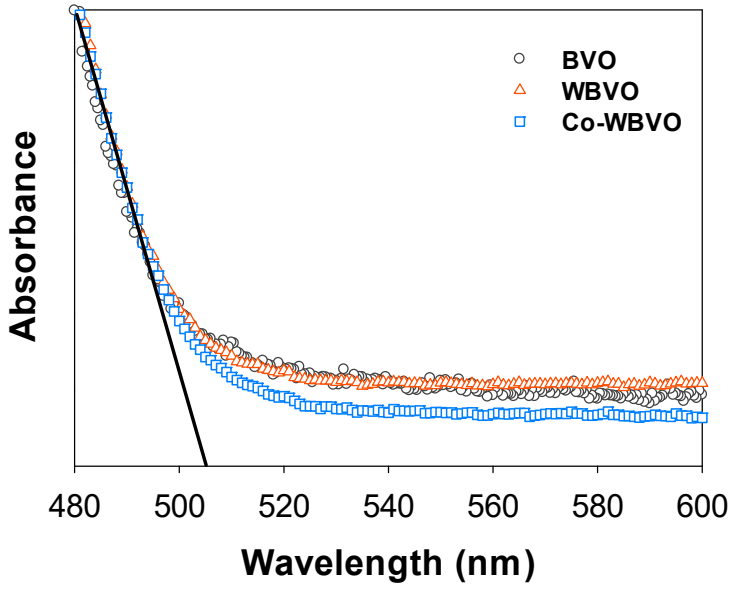

Fig. S6. UV-Vis diffuse reflectance absorption spectra of BVO, WBVO, Co-WBVO films.

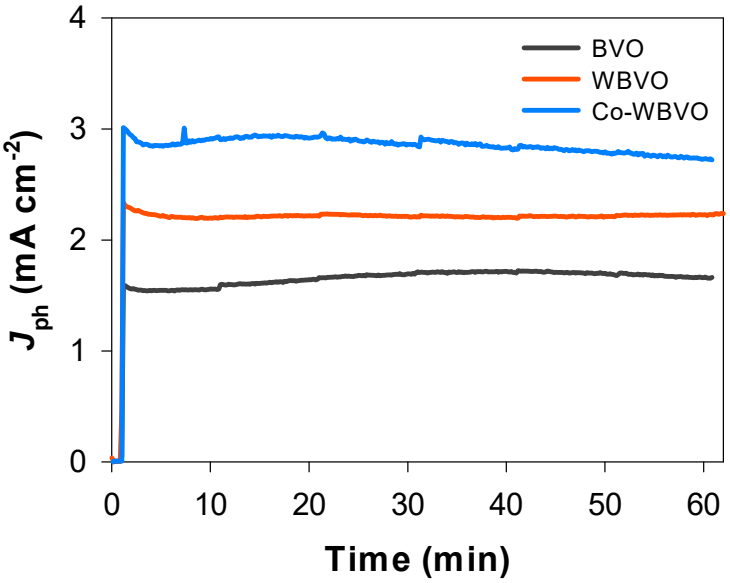

Fig. S7. Time-profiled J_{ph} changes at E = 1.36 V_{RHE} (0.73 V_{SCE}) in 0.171 M NaCl under AM 1.5 (100 mW cm^{-2}).

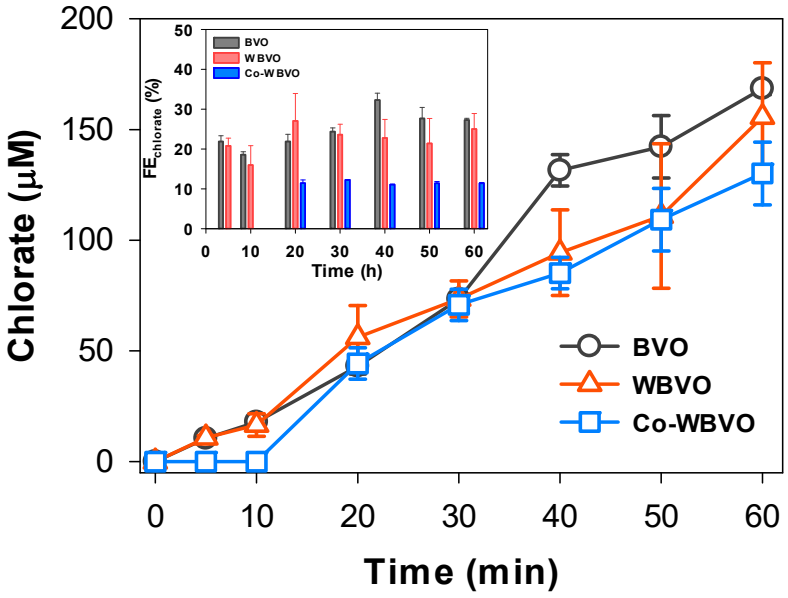

Fig. S8. Chlorate production during photoelectrochemical chloride oxidation using bare and modified BVO electrodes at E = 1.36 V vs. RHE in 0.171 M NaCl under 1 sun.

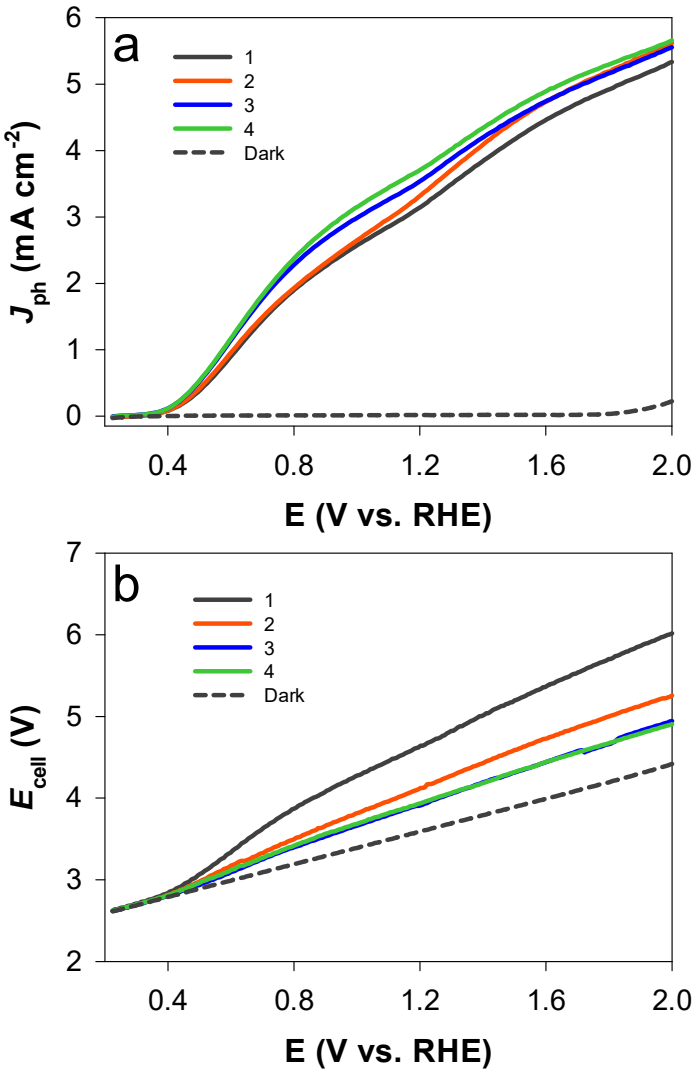

Fig. S9. (a) Linear sweep voltammograms with Co-WBVO photoanode coupled with different number of Na_xC electrode and (b) concurrent changes in E_{cell} of the Co-WBVO and Na_xC array pairs as a function of number of Na_xC electrode in 0.171 M NaCl under 1 sun. Na_xC electrodes were connected in parallel.

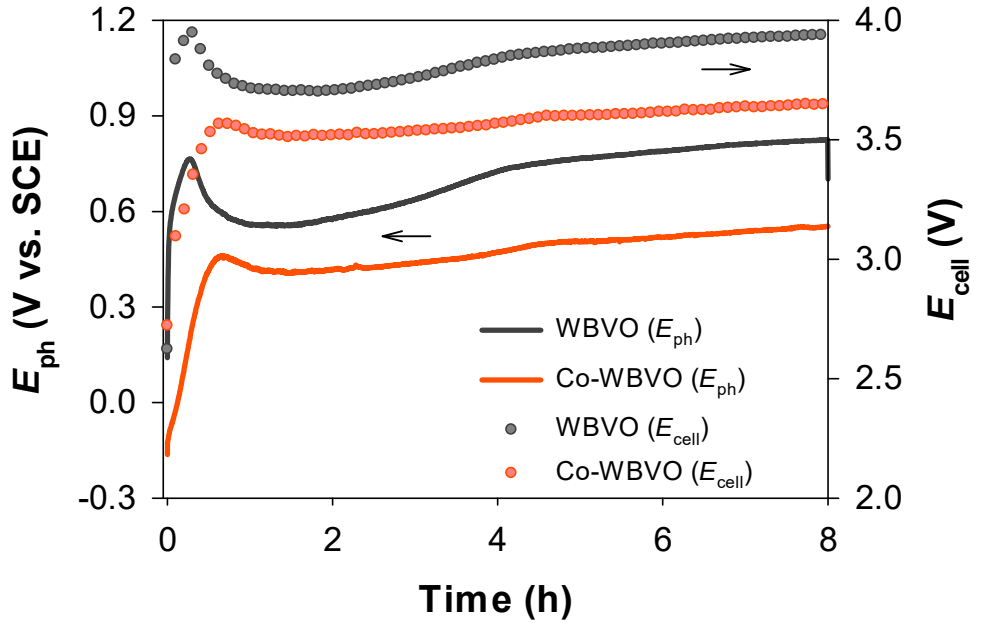

Fig. S10. Changes in the photopotential (E_{ph}) of WBVO and Co-WBVO photoelectrode coupled to Na_xC electrode in 0.171 M NaCl containing As(III) (1 mM) and NH_3 (1 mM) under 1 sun. While J_{ph} of 1 mA cm^{-2} was constantly maintained to the photoelectrodes, E_{cell}s of the photoelectrode and Na_xC electrode pairs were recorded. Note that the solution pH changed with time and hence the SCE scale was used.

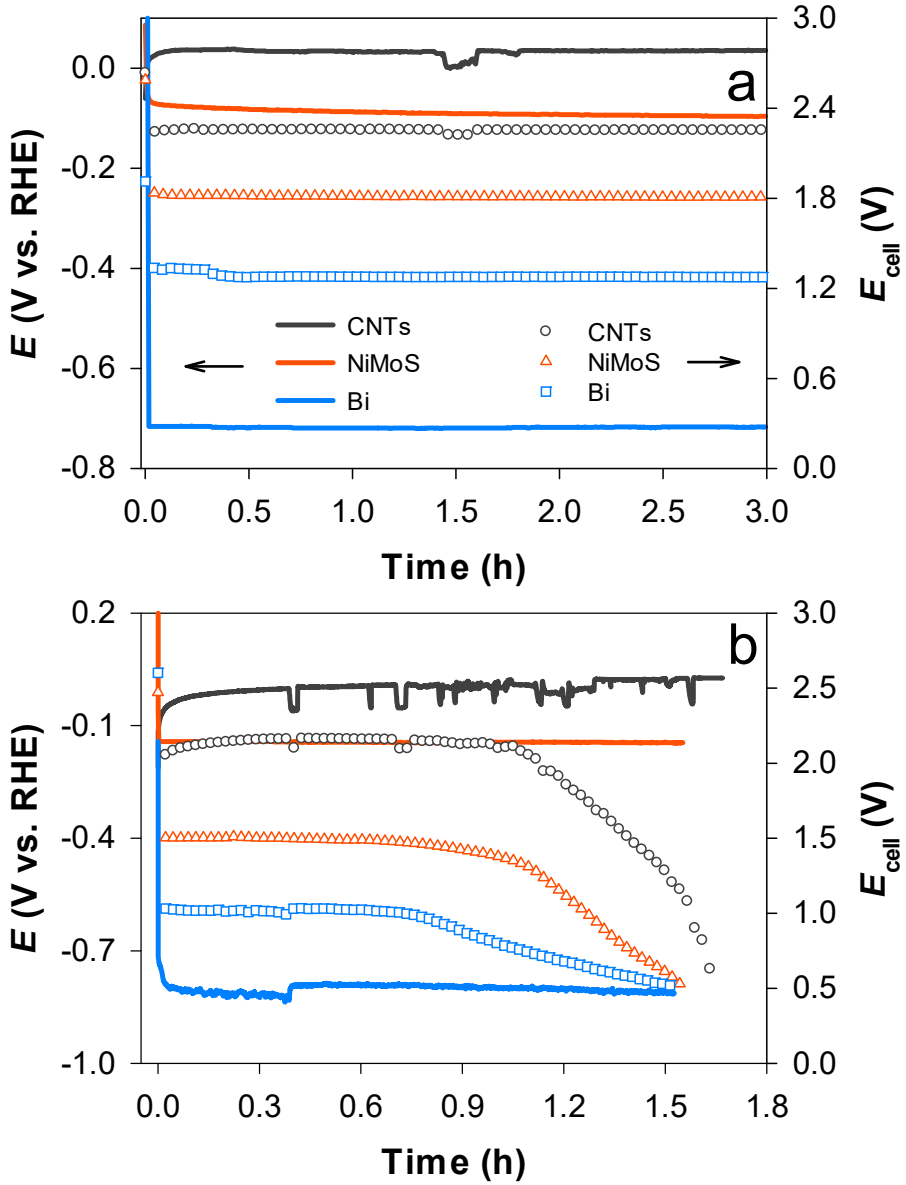

Fig. S11. Changes in discharging potentials (V vs. RHE) of CNTs, NiMoS, and Bi connected to the charged Na_xC with 8 mAh in 0.1 M K_2SO_4 (pH 6.5) purged with O_2, 0.1 M KOH (pH 13) purged with N_2, and 0.1 M $KHCO_3$ (pH 6.8) purged with CO_2, respectively. Constant J values of (a) −1 mA cm^{-2} and (b) −3 mA cm^{-2} were applied to the electrocatalysts, while E_{cell}s of the electrocatalyst and Na_xC pairs were recorded.

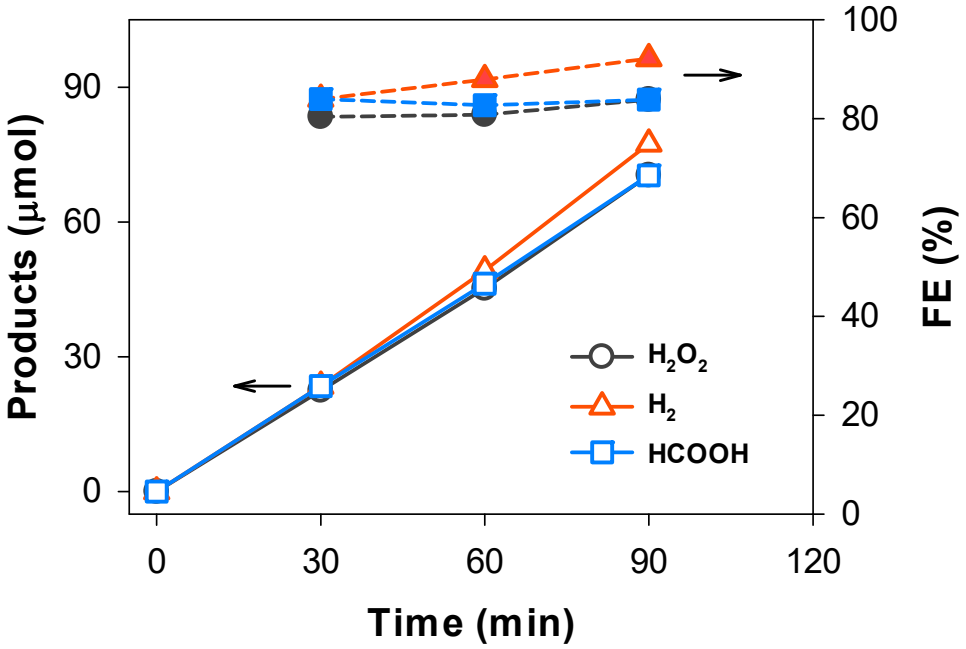

Fig. S12. Simultaneous productions and FEs of H_2O_2 via O_2 reduction with CNTs, H_2 via water reduction with NiMoS, and HCOOH via CO_2 reduction with Bi during the discharging stages. $J = -3$ mA cm^{-2}. See Fig. S11 for experimental conditions.

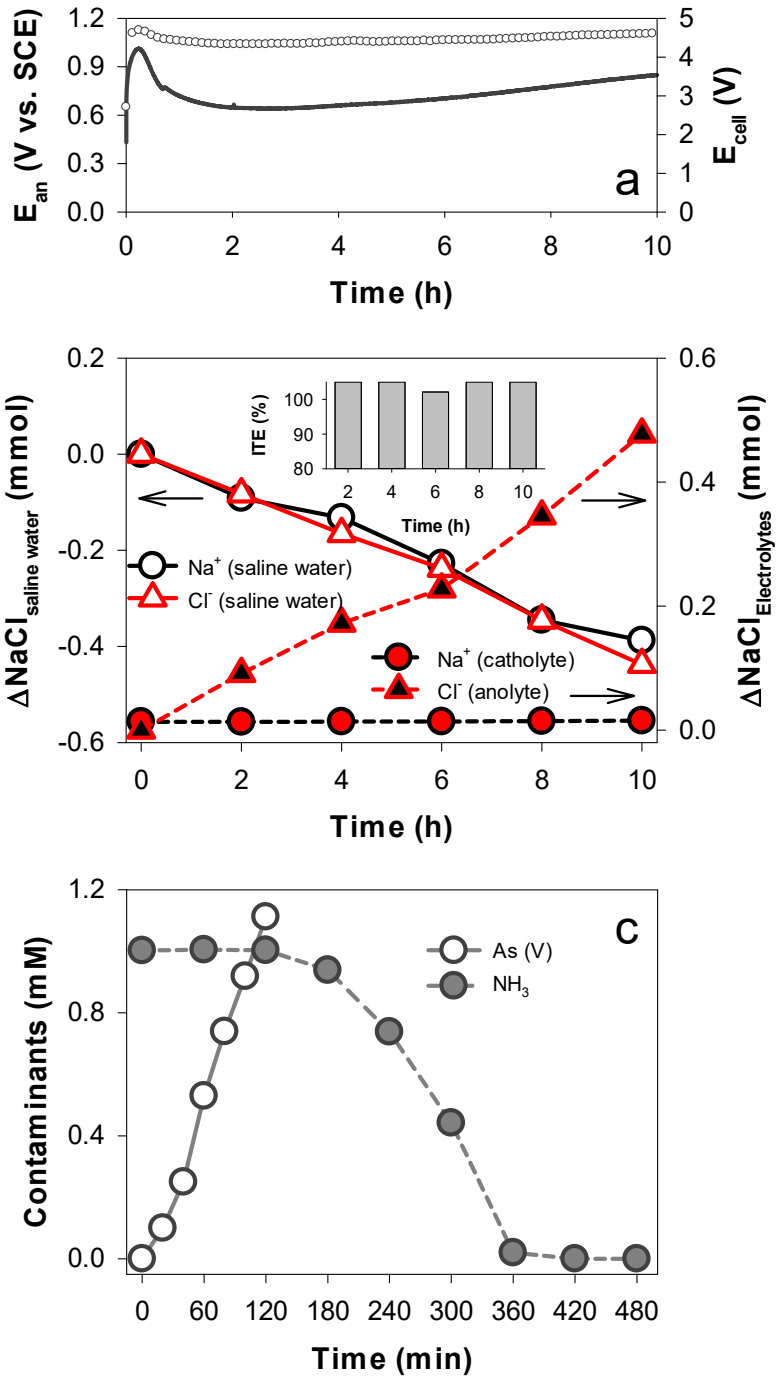

Fig. S13. A solar charging process with desalination of saline water (0.171 M NaCl) and oxidation of water contaminants (mixed As(III) and NH_3, each 1 mM). A WBVO photoelectrode (with SCE electrode) and Na_xC electrode were immersed in 0.171 M NaCl solutions. See **Scheme 1b** for the experimental setup. (a) Changes in E_{ph} of WBVO, and E_{cell} of WBVO and Na_xC pair at J_{ph} of 1 m A cm^{-2}. (b) Changes in the amounts of Na^+ and Cl^- in the saline water, Na^+ in the catholyte, and Cl^- in the anolyte. Inset shows ITEs. (c) Changes in As(V) and NH_3 concentrations.